01 Jan 1969

Fatigue testing of light gage metal forms

Kenneth W. Mouw

ENGINEERING
RESEARCH

ENGINEERING
RESEARCH

ENGINEERING
RESEARCH

ENGINEERING
RESEARCH

ENGINEERING
RESEARCH

SPECIAL REPORT

FATIGUE TESTING OF LIGHT GAGE METAL FORMS

Kenneth W. Mouw*

Civil Engineering

January 1969

*Supervised by Dr. C. E. Ekberg, Jr., Head, Department of Civil Engineering

ENGINEERING RESEARCH INSTITUTE
IOWA STATE UNIVERSITY AMES

ERI – 348
Project – 741

FATIGUE TESTING OF LIGHT GAGE METAL FORMS

INTRODUCTION

The fatigue strength of a composite slab with a light gage steel form was determined by testing a total of six specimens. Fatigue strength is assumed to be the highest applied load that a material can withstand for a specified number of cycles without failing. Each specimen in this project was a composite slab consisting of concrete and a light gage steel form. The composite slab incorporates a concept of coaction of concrete and steel which is dependent upon deformations of corrugated steel deck. Interaction between the deformations and the concrete slab causes the steel deck and the concrete slab to act as a composite unit under vertical loading. The six composite slab specimens were tested under fatigue loading to determine the range of repeated load which could cause failure after 1,000,000 cycles. Two different types of steel forms were tested. All of the specimens were subjected to the same minimum load but different maximum loads. Patterns and progressions of cracks were marked and load-deflection tests were conducted at intervals throughout the testing of each specimen.

DESCRIPTION OF THE TEST SPECIMENS

Six beam specimens were tested under fatigue loading. Two different types of forms were used in the testing which will be designated as Form I and Form R. Form I was used for two of the specimens. All six specimens were of the same basic dimensions: 72 in. long, 5 in. high, and

12 in. wide. Figure 1 shows a typical beam and its corresponding dimensions.

There are two types of deformations in the steel called indentations and embossments. Indentations are areas of metal protruding away from the concrete slab, and embossments are areas of metal protruding into the concrete slab. Form I uses only the embossments for coaction, and Form R uses both types of deformations. On Form I embossments are located on each web as shown in Fig. 2.

On Form R embossments are located on each web and along the center line of the bottom flange. The web embossments extend lengthwise along the deck sections. Indentations are centered on the top of each top flange. Figure 3 shows the location of the embossments and indentations for Form R.

MATERIALS

The specimens were cast in conjunction with the project "Investigation of Light Gage Steel Forms as Reinforcement for Concrete Slabs." The properties of the steel forms and the various batches of concrete were obtained from a progress report which was prepared for the sponsors of the project*.

The light gage steel forms were supplied by two different manufacturers. Both forms I and R have a minimum yield point of 33,000 psi and conform to ASTM A245-64 or A 446-64T.

---

*"Investigation of Light Gage Steel Forms as Reinforcement for Concrete Slabs," by M. L. Porter, R. M. Schuster, and C. E. Ekberg. Progress Report to American Iron and Steel Institute. Aug. 1, 1968.

The concrete was ordered from a local ready-mix plant to meet the following specifications:

1. 3,000 psi ultimate compressive strength in 7 days,
2. 3/8-in. maximum size aggregate except for the concrete batch cast on April 11, 1968 (cast number 3), which contained 3/4-in. maximum size aggregate, and
3. 3 in. slump.

More detailed information concerning the batches and the resulting compressive strengths is contained in Table 1, Appendix B.

FABRICATION, CASTING, AND CURING

Forms

All of the specimens were made with prefabricated steel forms supplied by the Economy Forms Company of Des Moines, Iowa.

Casting

A slump test was performed before casting the specimens. Usually two additional slump tests were made at approximately the one-third points during the pour. The amount of slump shown in Table 1 is the average of all slump tests performed for a particular casting date. Periodically during the pour, 6 x 12-in. waxed cardboard cylinder molds (control cylinders) were prepared according to ASTM specifications. Vibration of the concrete was performed on all the specimens, with a Stow Concrete Vibrator.

Curing

The concrete was cured for about 4 to 5 hours at room temperature, after which the control cylinders and the specimens were covered with wet burlap. Three days later the forms were stripped and the specimens were recovered with the wet burlap. The specimens were moist-cured for 7 days by rewetting the burlap and then air cured (dry) until tested. A covering of plastic film was kept over the wet burlap to reduce evaporation.

FATIGUE TESTING SYSTEM

An MTS Electro-Hydraulic Structural Loading System was used to apply the fatigue loading to the specimens. The system consists of a number of interconnected components shown in Fig. 4. The majority of the system's electronic units are located in a control console and are interconnected to make up the electronic control function. External to the console are the hydraulic actuator and the hydraulic power supply, which furnishes fluid energy to the actuator.

Theory of Operation

A closed loop electro-hydraulic servo system is designed to provide precise control of loads imposed on a specimen to acquire information about the behavior of the specimen under the fatigue loading conditions.

The basic theme of the closed-loop control system is the comparison of the desired condition of a controlled load with the actual condition of the load and the resultant generation of correction signals that causes the actual condition to equal the desired condition. Implementation of this idea is easily accomplished by using electronic signals to represent the desired condition (command), the actual condition (feedback), and the correction signal (difference).

Whenever a difference between two signals occurs, the detected difference is amplified and this amplified signal is used to control the servo valve. The servo valve controls hydraulic flow to the actuator, which determines the force acting on the specimen. As the actual condition of the specimen nears the desired condition, the difference between command and feedback signals is reduced and proportionally smaller signals are sent to the servo valve. This action continues until the command and feedback signals are equal. Once these two signals are the same, the control circuits will maintain this relationship within the accuracy limits of the system. The cyclic loading pattern is diagrammed in Fig. 5.

Placement of Specimen

A close-up of how the specimen was supported on a steel frame is shown in Fig. 1. This close-up also shows how the load from the actuator was applied to the specimen. The table in Fig. 1 indicates the distances to the points of loading for the specimens tested.

Calibration

A 20,000 lb Baldwin dynamometer was used to check the accuracy of the MTS loading system. This check was done by observing actual loads from the dynamometer and correlating these to the loads observed from the

MTS loading system. At low loads there was a significant difference, but as the load increased the difference decreased.

PROCEDURE OF TESTING

The test procedure involved static and fatigue testing. At the beginning of each beam test a repeated load range was specified that presumably would cause fatigue failure after 1,000,000 cycles. The minimum total load, in each case, was 400 lb and the maximum total load varied from 2,200 to 3,400 lb.

The first step in testing the specimen was to apply loads in 200 lb increments up to the maximum total load. At each increment in load, midspan deflections were recorded. While the maximum load was being applied, the specimen was thoroughly checked for any cracks that may have developed. The cracks were marked with a felt pen marker.

After this initial load-deflection test, the load was reduced to a median value. From this median load the specimen was subjected to cycling from a minimum load to a maximum load until failure occurred, see Fig. 5. Additional load-deflection tests were performed at intervals of 100,000 or 200,000 cycles.

Some of the specimens were cycled past what was later determined as the failure point, because at the beginning of the testing there was not any definite criteria for failure. Failure was established to be at the point when the bond between the metal form and the concrete was lost, a major crack developed, end-slip occurred, and the deflection increased markedly.

Even after the fatigue failure, the friction between the embossments on the steel form and the concrete was great enough to withstand a still larger load. The maximum load that was obtained in a static test after the fatigue failure was considered to give the ultimate moment.

EXPLANATION OF NOMENCLATURE

The following symbols were used for a fatigue test specimen:

I or R = light gage steel form used.

An example of the proper designation for a specimen would be as follows:

I-1-3-77

where: I = form I was used

1 = test number 1

3 = casting number (cast number 3 was made on April 11, 1968)

77 = number of days elapsed from casting to failure.

An abbreviation for I-1-3-77 is I-1.

TEST RESULTS

The test results are divided into sections according to the specimen involved. In each section several things are discussed, including load-deflection, deflection versus cycles, number and pattern of cracks, and stress and moment ratios.

Slab I-1-3-77

This was the first fatigue test, and it was necessary to guess at a load range which would cause fatigue failure at 1,000,000 cycles. On the basis of previous static tests the value of 2,200 lb was known to be greater than 50% of static ultimate load. It was decided to try a 2,200 lb maximum load with a minimum load of 400 lb. After 2,000,000 cycles there were no indications that a fatigue failure had occurred and the beam was statically loaded to M_{ult} of 3,600 ft-lb. The beam failed by complete loss of bond and friction between the concrete and the metal form. All of the test results are given in Tables 2 and 3, and Figs. 6, 7, 8, 9, and 10.

As shown in Table 2 the deflections at the maximum load were recorded periodically throughout the test. It can be seen from this table that at the low load range for I-1 there was a negligible increase in deflection after the first 100,000 cycles.

The bottom portion of Fig. 6 shows the plot for load versus midspan deflection. The greatest increase in deflections were during the first 100,000 cycles. The deflections were nearly proportional to the load. The slope of the load-deflection curve remained fairly constant as the number of cycles increased, indicating a constant stiffness of the specimen. The permanent set increased as the number of cycles increased. However at this low load range the increase in the permanent set was only about 0.01 in. after the first 100,000 cycles.

Figure 7 shows how the deflection for a specified load changed as the number of cycles increased. For I-1 the ratio of the maximum applied moment to the ultimate moment was less than 0.60 and there was no increase in deflection with an increase in the number of cycles.

The location and the height of all the cracks for I-1 and the other specimens can be seen in Fig. 8. The number beside the cracks in the figure indicates the number of cycles, in thousands, at which the progress of the crack was marked. After the first 100,000 or 200,000 cycles, the height of the cracks did not increase significantly. A plot of how the number of cracks increased with an increasing number of cycles can be seen in Fig. 9. As the number of cycles increased, an attempt was made to measure the increase in the width of the major crack for each specimen. However, the cracks were so small, less than 0.005 in., that available instruments for measuring were not accurate enough.

Tabulated in Table 3 are the ratios of the bending stresses at the top of the concrete to the compressive strength of the concrete and the bending stresses at the bottom of the steel to the ultimate strength of the steel. The ratios of the applied moments to the ultimate moment are also in Table 3. The ratio of the stresses versus the ratio of the moments for I-1 are plotted in Fig. 10.

Slab I-2-3-85

Using the same M_{ult} as was found for I-1, I-2 was statically loaded to 3,000 lb or an M/M_{ult} of 0.83, after which the slab was cycled with a minimum M/M_{ult} of 0.11 (400 lb) and a maximum M/M_{ult} of 0.78 (2,800 lb). After 601,120 cycles with no signs of a probable fatigue failure, the maximum M/M_{ult} was increased to 0.89 (3,200 lb). At 909,500 cycles the specimen was accidentally failed during a static load-deflection test. All of the test results are given in Tables 2 and 3, and Figs. 6, 7, 8, 9, and 10.

In Table 2 it can be seen that the maximum deflection increased only 0.007 in. between 100,000 cycles and 601,000 cycles. It was because of this very small increase that at 601,000 cycles the maximum load was increased to 3,200 lb. After the load increase the deflections increased more rapidly.

From the top of Fig. 6 it can be seen that between 100,000 and 600,000 cycles the stiffness remained constant as seen from the slopes of the load-deflection curves. However, after 600,000 cycles, the increased load did start to cause a decrease in stiffness.

Figure 7 shows that the first 600,000 cycles caused an increase in deflections of 0.007 in. After 600,000 cycles the deflections were much larger as the number of cycles increased.

The location and height of the cracks in slab I-2 are shown in Fig. 8. . There were more cracks in I-2 than I-1 because of the higher moments that were applied. The increase in the number of cracks with an increasing number of cycles is shown in Fig. 9.

The ratio of the bending stresses to the moment ratios are tabulated in Table 3 and plotted in Fig. 10. Also tabulated in Table 3 are the cyclic loading values and the specimen properties.

Slab R-1-4-

Before testing slab R-1 a corner of the concrete was accidentally broken. The shear span of 24 in. was maintained but the middle constant moment span was reduced to 14 in. The testing of slab R-1 was begun with a moment of 3,200 ft-lb; this was because slab I-2 showed signs of being capable of withstanding a moment comparable to this value. The slab failed catastrophically at 350,000 cycles. There are doubts as to the validity of the failure because it was catastrophic.

All the test results for R-1 are given in Tables 3 and 4, and Figs. 8, 9, 11, 12, and 13.

The load-deflection relationship for various points in the cycling are plotted in Fig. 11. From the bottom of this figure it can be seen why the validity of this failure of R-1 is doubted. The increase in deflection between 50,000 and 300,000 cycles is very small, and no signs of an impending failure are evident.

The maximum deflections that were recorded periodically throughout the test are tabulated in Table 4. In this particular instance the maximum deflections coincide with the values plotted in Fig. 12 for R-1. In Fig. 12 it is also evident that a failure was not expected.

Figure 8 shows the location and height of the cracks in R-1, and Fig. 9 shows the relatively small number of cracks as the number of cycles increased.

The ratios of the applied moments to the ultimate moment, the bending stresses at the top of the concrete to the compressive strength of the concrete, and the bending stresses at the bottom of the steel to the ultimate strength of the steel are tabulated in Table 3.

The stress ratios are plotted against the moment ratios in Fig. 13.

Slab R-2-6-21

The initial loading range for R-2 was the same as R-1, with a minimum 400 lb and a maximum 3,200 lb. After 2,000,000 cycles the maximum load was increased to 3,400 lb. Between 2,800,000 and 3,000,000 cycles end-slip occurred and a major crack developed, but the beam withstood the maximum load. At 3,000,000 cycles the load during a static load test was increased to 4,100 lb which gave an ultimate moment of 4,100 ft-lb before complete collapse occurred.

The stiffness of R-2 as shown in Fig. 11 remained constant throughout the test, until the fatigue failure at 3,000,000 cycles. The stiffness did not change when the load was increased but did decrease slightly after the fatigue failure.

Figure 12 shows how the deflections at a specified load increased steadily as the number of cycles increased. After 2,800,000 cycles there was a large increase in the deflection and it was at this point that failure occurred.

Results for R-2 are also shown in Tables 3 and 4, which include the maximum deflections at the maximum loads at various intervals in the cycling and the specimen loading characteristics. Figures 8, 9, and 13 show the height and pattern of the cracks, the number of cracks with an increasing number of cycles, and the ratio of the bending stresses to the moment ratios.

Slab R-3-5-34

It was initially decided to try slab R-3 at a loading range of 400 to 3,400 lb on basis of experience with slab R-2. However, during the initial static loading of R-3, a major crack accompanied by end-slip formed at 3,200 lb and the load was not increased above this value. Although there was end-slip and a major crack in the slab, which would constitute a failure, the slab was subjected to 600,000 cycles of loading. This produced additional end-slip of a progressive nature. After the 600,000 cycles the specimen was statically loaded to an ultimate moment of 4,700 ft-lb.

In Fig. 11 for slab R-3 it can be seen that a very large increase in deflection had occurred between 3,000 and 3,200 lb of load during the initial static test. Also shown are the very large deflections of slab R-3 after 50,000 cycles, which are comparable to those of slab R-2 after its fatigue failure.

Slab R-4-6-33

For slab R-4 it was again decided to try a loading range of 400 to 3,400 lb, which met with more success than the previous slab R-3.

Between 200,000 and 243,000 cycles end-slip occurred indicating a fatigue failure. At 450,000 cycles the slab was statically loaded to a maximum load of 4,200 lb.

Figure 11 shows that the deflections for slab R-4 after fatigue failure were comparable to those of slab R-2 after its fatigue failure. At a static load of 3,400 lb the deflections were 0.240 to 0.296 in. for R-4 and R-2 respectively.

CONCLUSIONS

Of the six specimens subjected to fatigue loading there were two definite fatigue failures, and both of these were with Form R. The cyclic load ranges varied from a minimum of 0.09 M/M_{ult} to a maximum of 0.89 M/M_{ult}. The number of cycles required to cause a failure ranged from one cycle, a beam that failed during its initial static load test, to 2,800,000 cycles.

Slab R-2 was cycled for 2,000,000 cycles at a maximum stress ratio of 0.30 in the concrete, which is the ratio of the stress in the top fiber of the concrete to the compressive strength (f'_c) of the concrete, and a maximum stress ratio of 0.45 in the steel, which is the ratio of the stress in the bottom fiber of the steel to the ultimate strength of the steel. After 2,000,000 cycles the maximum stress ratio, 0.32 in the concrete and 0.47 in the steel, was increased for an additional 800,000 cycles before failure occurred. This was comparable to a load range of 0.09 M/M_{ult} to 0.78 M/M_{ult}. Slab R-4 was cycled for 200,000 cycles at a maximum stress ratio of 0.32 in the concrete and 0.47 in the steel before failure occurred.

The repeated bending stresses in the steel and concrete for the two specimens which failed in fatigue were not severe enough to cause fatigue in the concrete and steel. The fatigue failure was caused by the loss of composite action between the concrete and the metal form. When the bond between the metal form and the concrete was lost, a major crack developed, end-slip occurred, and the deflection increased markedly. Although a fatigue failure had occurred, the friction between the embossments on the steel form and the concrete was great enough to withstand a higher load. The higher load was comparable to ultimate loads performed on other specimens under static loading.

There were four specimens tested which did not fail in fatigue because of various reasons. There were no signs of an impending fatigue failure, at 2,000,000 cycles, for I-1 because of the low maximum stress ratio, 0.19 in the concrete and 0.26 in the steel.

With a maximum stress ratio of 0.28 in the concrete and 0.38 in the steel, slab I-2 was starting to show signs of an approaching fatigue failure at 900,000 cycles, but it was inadvertently failed during a static load-deflection test.

Slab R-1 was tested at a maximum stress ratio of 0.36 in the concrete and 0.45 in the steel. At 300,000 cycles there were no indications of an imminent fatigue failure, however at 350,550 cycles there was a catastrophic failure. The validity of this test is doubtful because of the dramatic failure.

Specimen R-3 was failed by end-slip during its initial static load-deflection test at a stress ratio of 0.35 in the concrete and 0.45 in the steel.

The stiffness of the specimens, except after failure, remained fairly constant throughout the testing. After failure there was a noticeable decrease in the stiffness because of the loss of composite action.

The permanent set at the maximum loads in the specimens increased the most during the first 100,000 cycles, about 0.08 in., and after a major crack had formed, about 0.24 in. After the first 100,000 cycles, the rate of increase in the permanent set decreased with an increasing number of cycles.

The majority, usually about eight, of the cracks in the slabs tested developed during the initial static load deflection test or else during the first 100,000 cycles. The height of the cracks did not increase much after the first 100,000 cycles. The cracks were close to 3 in. apart and fairly vertical until they reached into the compression zone, at which time they became more diagonal.

RECOMMENDATIONS

More accuracy is needed on the end-slip observations. A method should be devised to more accurately determine when the end-slip occurs.

On future specimens load-deflection tests should be conducted at lower increments as follows:

1 cycle

10 cycles

100 cycles

1,000 cycles

10,000 cycles

100,000 cycles

To provide more uniformity in the test results a larger number of specimens should be from the same casting.

SOURCES OF MATERIAL

Inland Floor Systems: Catalog No. 270, Inland Steel Products Co., Milwaukee, Wisconsin, 1968.

MTS Division: Instruction Manual for Model 900.82 Electro-Hydraulic Structural Loading System, MTS Division, Minneapolis, Minnesota, 1965.

Porter, M. L., Schuster, R. S., and Ekberg, C. E. Investigation of Light Gage Steel Forms as Reinforcement for Concrete Slabs, Engineering Research Institute, Ames, Iowa, 1968.

Q-Floor Q-Air Floor Q-Lock Floor, H. H. Robertson Co., Pittsburg, Pa., 1968.

APPENDIX A — GENERAL NOMENCLATURE

ASTM	American Society for Testing Materials
Av	Average
f_c	Stress in the top fiber of the concrete
f'_c	Compressive strength of concrete in psi
f_s	Stress in the bottom fiber of steel
f'_s	Ultimate strength of steel in psi
ft-lb	Foot-pound
gal	Gallon
in.	Inch
I_t	Transformed moment of inertia of composite slab in inches to the fourth power
kip	One thousand pounds
lb	Pounds
M	Moment
Max	Maximum
Min	Minimum
M_{max}	Maximum moment
M_{min}	Minimum moment
M_{ult}	Ultimate moment obtained by averaging the ultimate moments that beams could withstand after fatigue testing
No.	Number
P_{max}	Maximum load
P_{min}	Minimum load
psi	Pounds per square inch
vs	versus

APPENDIX B — TABLES

Table 1. Summary of concrete properties used in casting specimens.

Date of casting	Casting number	Cement properties[c], sacks/yd	Fine, lb/yd	Coarse, lb/yd	Max size, in.	Water added[b], gal/yd	Slump[a], in.	Compressive strength f'_c	Age of f'_c, days	Modulus of rupture, psi	Age of modulus of rupture, days
4/11/68	3	5	1466	1868	3/4	27.7	2 3/4	3908	37	611	50
6/21/68	4	5	1648	1784	3/8	33.0	3 1/2	2956	12	–	–
6/27/68	5	5	1645	1790	3/8	27.0	3 1/2	3103	22	–	–
7/5/68	6	6	1560	1707	3/8	32.0	5	3708	22	–	–

(a) No admixtures were added to any concrete castings.

(b) Water added includes only that added at plant plus water added on truck.

(c) Cement used for all concrete castings was Type 1 of Northwestern brand.

Table 2. Experimental results for Form I.

Beam No.	No. of cycles	Max load, lb	Max deflection, in.
I-1-3-77	0	2000	0.026
	103,340	2200	0.044
	200,000	2200	0.051
	300,000	2200	0.051
	400,000	2200	0.051
	500,000	2200	0.046
	1,000,000	2200	0.050
	1,250,300	2200	0.046
	1,500,160	2200	0.043
	2,000,000	2200	0.049
	Static ultimate	3600	0.085
I-2-3-85	0	3000	0.046
	100,000	2800	0.070
	200,000	2800	0.074
	300,000	2800	0.075
	500,000	2800	0.075
	601,121	2800	0.077
	601,121	3200	0.084
	803,840	3200	0.093
	909,500	3200	0.104

Table 3. Summary of test data.

Beam No.	Load[(a)], lb Min	Load[(a)], lb Max	Moment (M), ft-lb Min	Moment (M), ft-lb Max	Ultimate moment (M_{ult}), ft-lb	No. of cycles	I_{t_4}, in.	I_{t_4}/n, in.	kd, in.	f'_c, psi	f'_s, psi
I-1	400	2200	400	2200	3600	2,000,000	51.706	6.396	1.463	3908	55,300
I-2	400	2800	400	2800	3600[(b)]	600,000	51.706	6.396	1.463	3908	55,300
I-2	400	3200	400	3200	3600[(b)]	300,000	51.706	6.396	1.463	3908	55,300
R-1	400	3200	400	3200	4333[(c)]	350,000	55.880	5.569	1.557	2956	52,400
R-2	400	3200	400	3200	4333[(c)]	2,000,000	51.426	5.747	1.509	3700	52,400
R-2	400	3400	400	3400	4333[(c)]	1,300,000	51.426	5.747	1.509	3700	52,400
R-3	400	3200	400	3200	4333[(c)]	600,000	54.949	5.605	1.563	3103	52,400
R-4	400	3400	400	3400	4333[(c)]	450,000	51.426	5.747	1.509	3700	52,400

[(a)] All tests were done with an MTS Electro-Hydraulic Structural Loading System.

[(b)] From test on I-1.

[(c)] Average from tests on I-2, I-3, and I-4.

Beam No.	Bending stresses: Top fiber of concrete f_{cmin}, ksi	Bending stresses: Top fiber of concrete f_{cmax}, ksi	Bending stresses: Bottom fiber of steel f_{smin}, ksi	Bending stresses: Bottom fiber of steel f_{smax}, ksi	Stress ratio: Top fiber $\frac{f_{cmin}}{f'_c}$	Stress ratio: Top fiber $\frac{f_{cmax}}{f'_c}$	Stress ratio: Bottom fiber $\frac{f_{smin}}{f'_s}$	Stress ratio: Bottom fiber $\frac{f_{smax}}{f'_s}$	Moment ratio $\frac{M_{min}}{M_{ult}}$	Moment ratio $\frac{M_{max}}{M_{ult}}$
I-1	0.136	0.748	2.654	14.599	0.0348	0.1914	0.0480	0.2640	0.1111	0.6111
I-2	0.136	0.952	2.654	18.581	0.0348	0.2436	0.0480	0.3360	0.1111	0.7777
I-2	0.136	1.088	2.654	21.235	0.0348	0.2784	0.0480	0.3840	0.1111	0.8888
R-1	0.134	1.069	2.971	23.766	0.0453	0.3616	0.0567	0.4535	0.0923	0.7385
R-2	0.141	1.126	2.916	23.325	0.0381	0.3043	0.0556	0.4451	0.0923	0.7385
R-2	0.141	1.197	2.916	24.783	0.0381	0.3235	0.0556	0.4730	0.0923	0.7846
R-3	0.136	1.091	2.943	23.546	0.0438	0.3516	0.0562	0.4494	0.0923	0.7385
R-4	0.141	1.197	2.916	24.783	0.0381	0.3235	0.0556	0.4730	0.0923	0.7846

Table 4. Experimental results for Form R.

Beam No.	No. of cycles	Max load, lb	Max deflection, in.
R-1-4-17	0	3200	0.053
	50,000	3200	0.083
	100,800	3200	0.086
	300,480	3200	0.089
R-2-6-21	0	3200	0.101
	100,000	3200	0.125
	200,600	3200	0.145
	250,000	3200	0.145
	300,140	3200	0.147
	400,000	3200	0.149
	450,000	3200	0.147
	500,000	3200	0.151
	700,000	3200	0.154
	800,000	3200	0.156
	1,000,000	3200	0.164
	1,100,000	3200	0.163
	1,287,400	3200	0.168
	1,403,540	3200	0.171
	1,501,480	3200	0.171
	1,700,000	3200	0.174
	2,000,000	3200	0.175
	2,100,000	3400	0.176
	2,300,730	3400	0.183
	2,400,000	3400	0.184
	2,500,780	3400	0.185
	2,701,300	3400	0.186
	2,800,000	3400	0.187
	3,000,000	3400	0.192
	3,050,000	3400	0.295
	3,100,130	3400	0.317
	3,250,660	3400	0.346
R-3-5-34	0	3000	0.092
	0	3200	0.176
	50,000	3200	0.262
	200,000	3200	0.290
	301,120	3200	0.364
	400,000	3200	0.494
	600,000	3200	0.492
R-4-6-33	0	3400	0.090
	200,000	3400	0.166
	243,000	3400	0.241
	401,460	3400	0.259
	450,000	3400	0.260

APPENDIX C — FIGURES

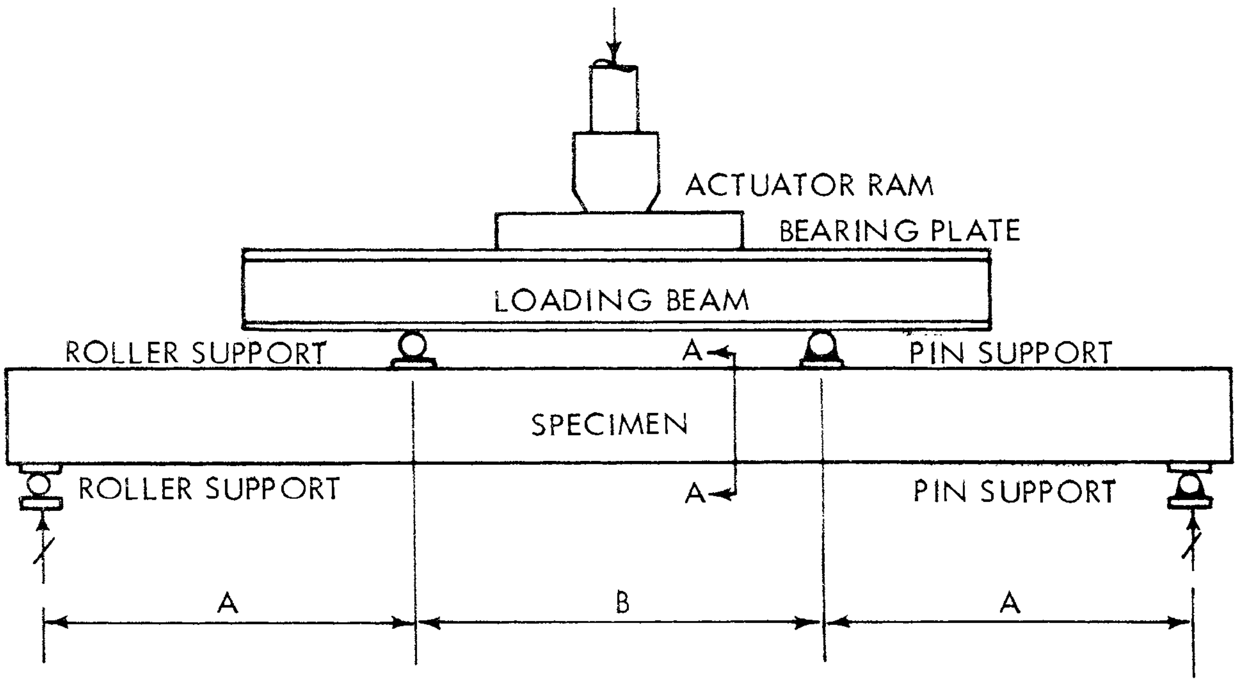

BEAM	A, in.	B, in.
FI1	24	20
FI2	24	20
FR1	24	14
FR2	24	20
FR3	24	20
FR4	24	20

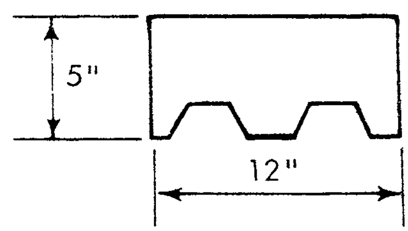

A–A

Fig. 1. Specimen support and loading arrangement.

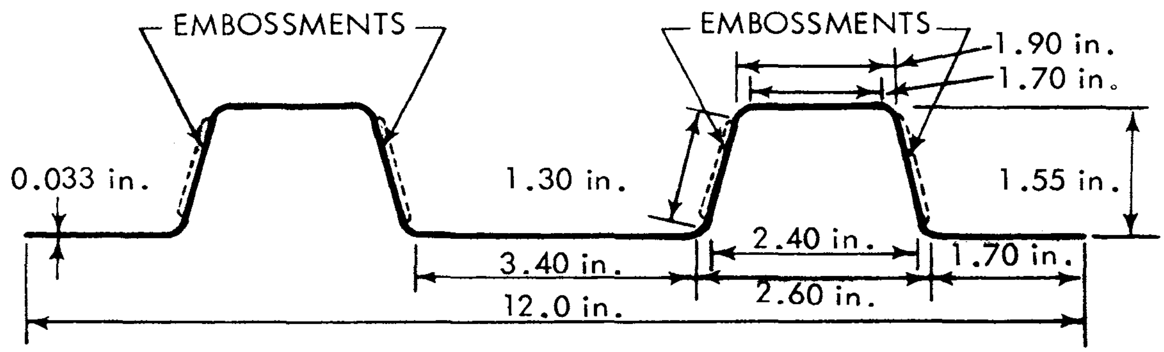

Fig. 2. Typical cross section of Form I.

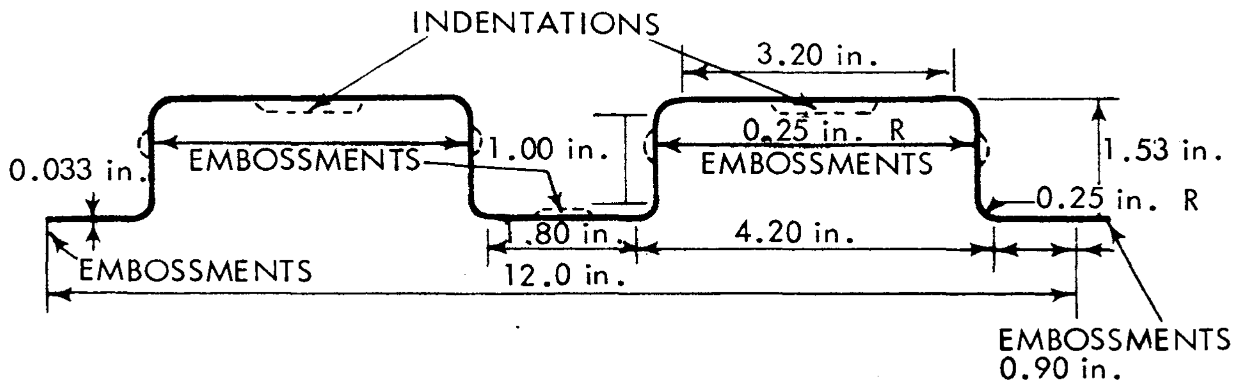

Fig. 3. Typical cross section of Form R.

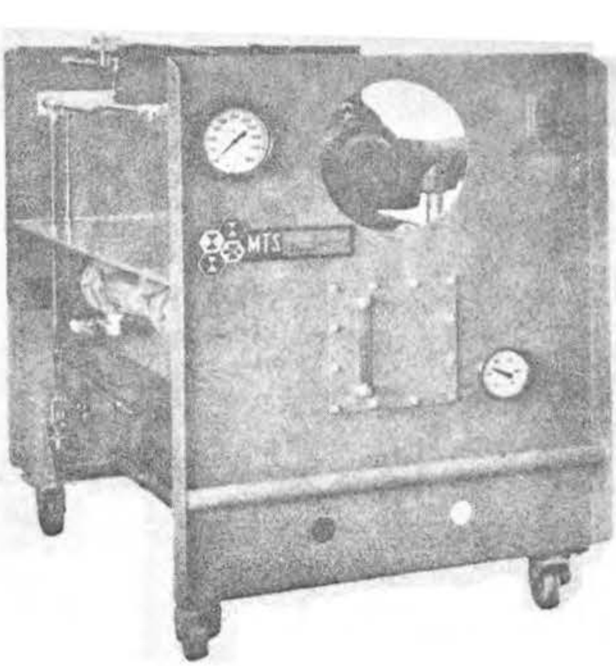

Hydraulic power supply

Hydraulic actuator

Control console

Fig. 4. Model 900.82 electro-hydraulic structural loading system.

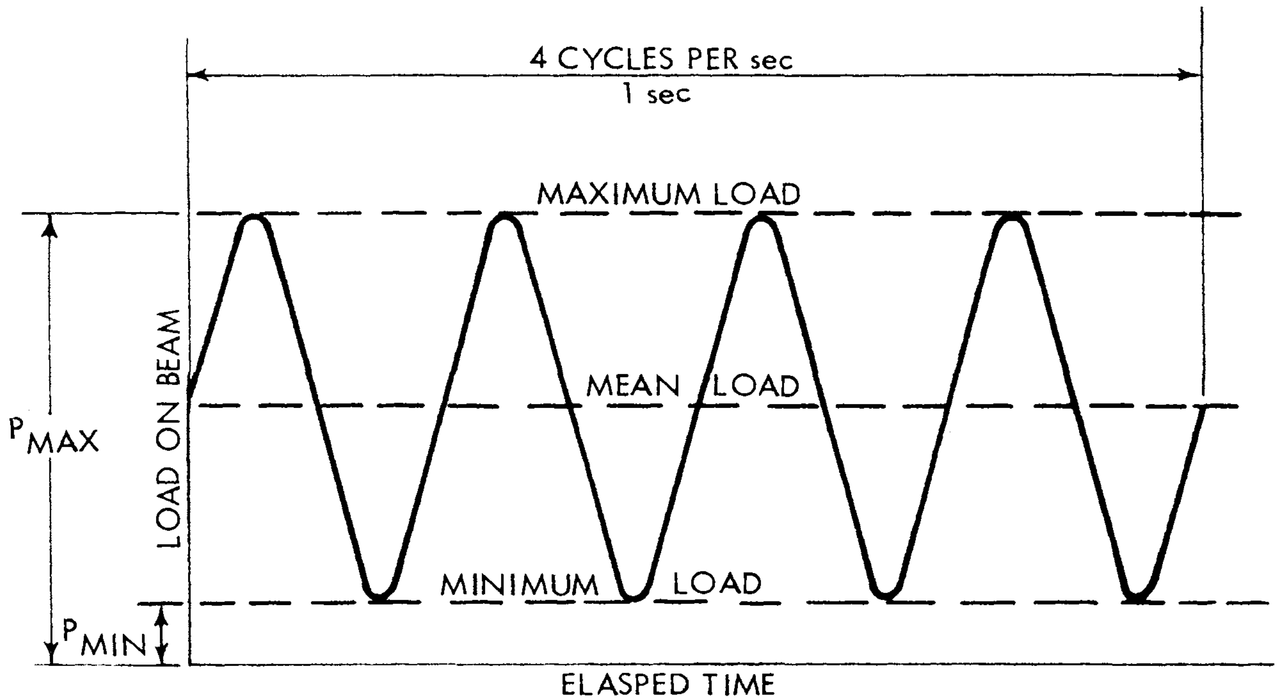

Fig. 5. Cyclic loading pattern.

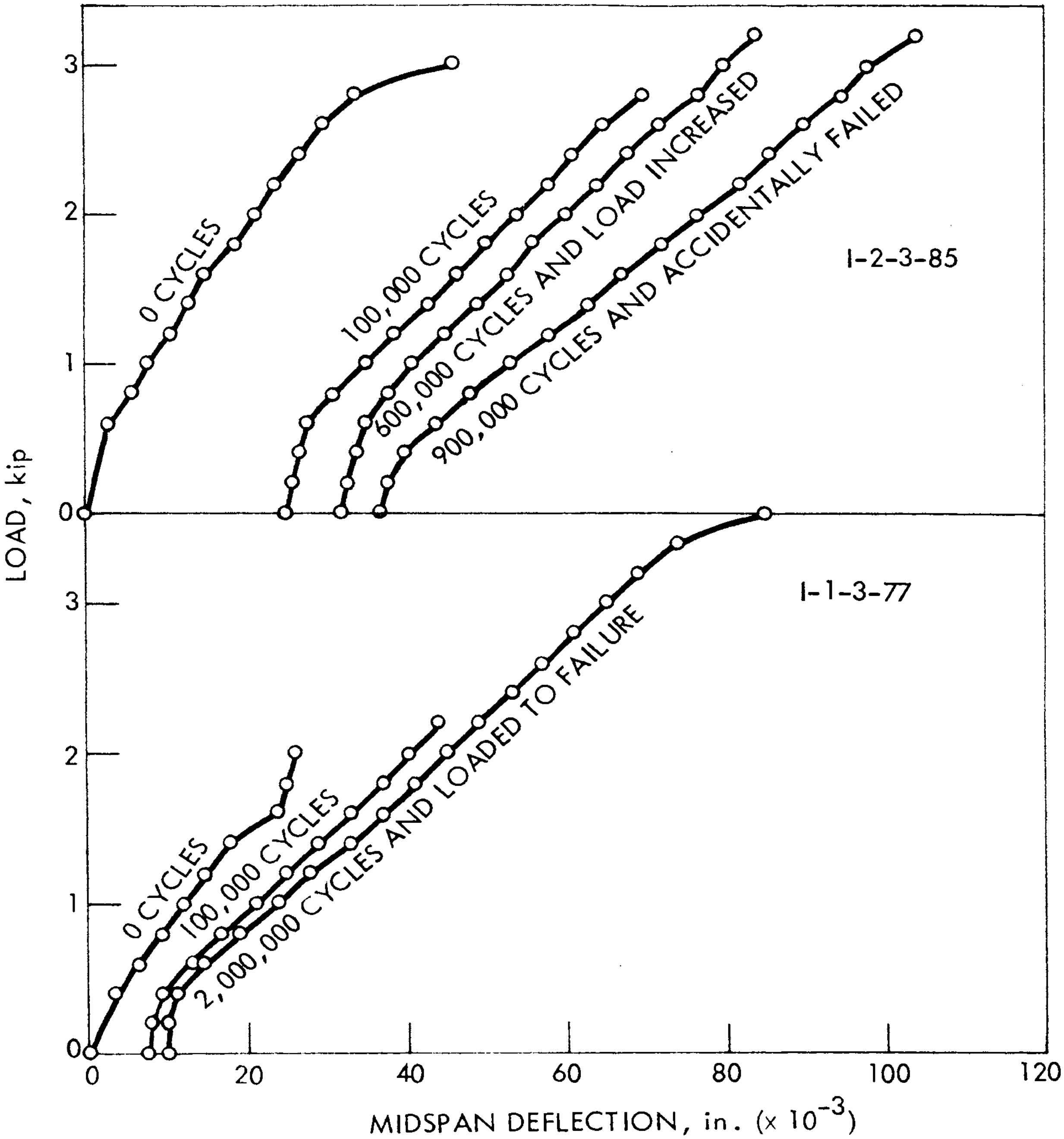

Fig. 6. Load vs midspan deflection for static tests.

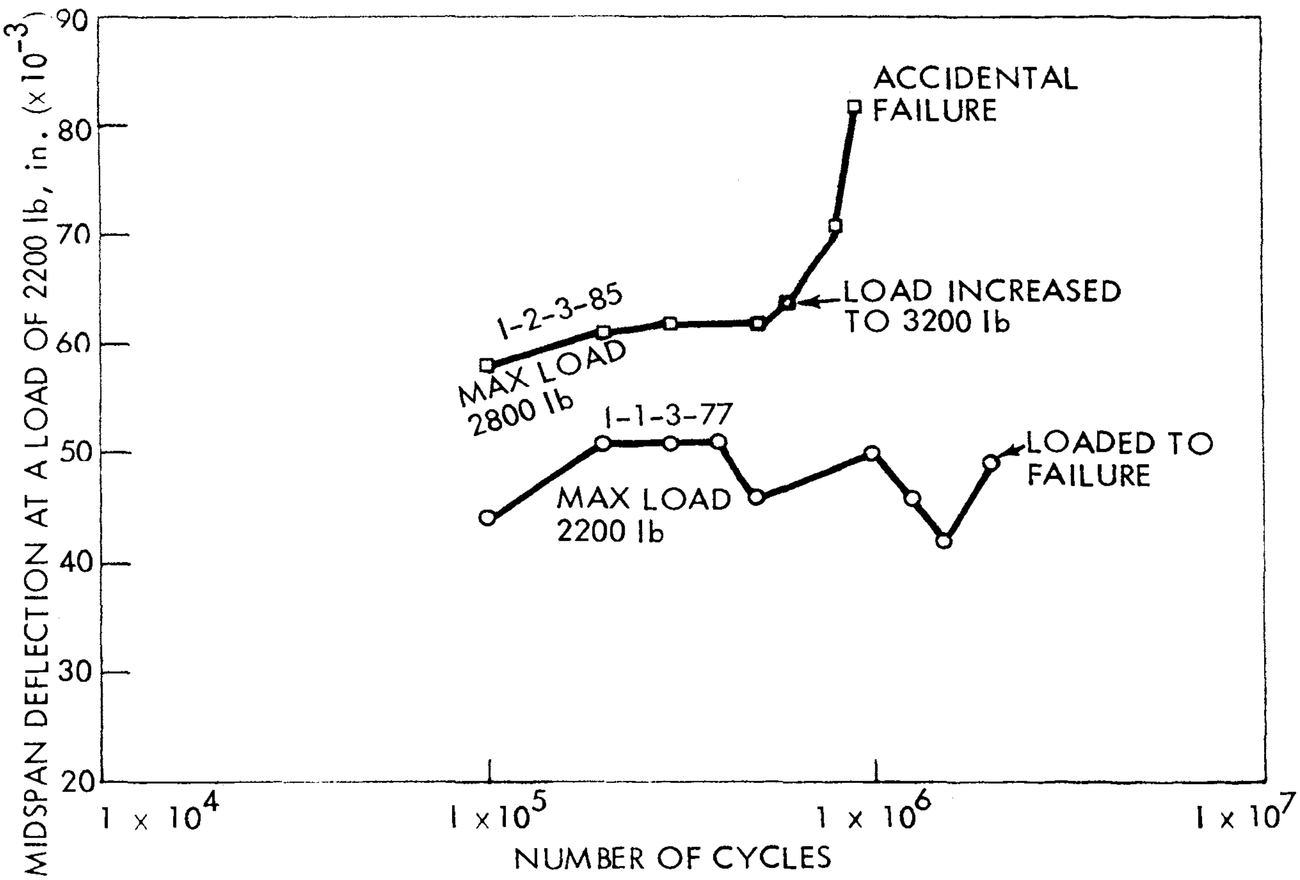

Fig. 7. Midspan deflection vs number of cycles for Form I.

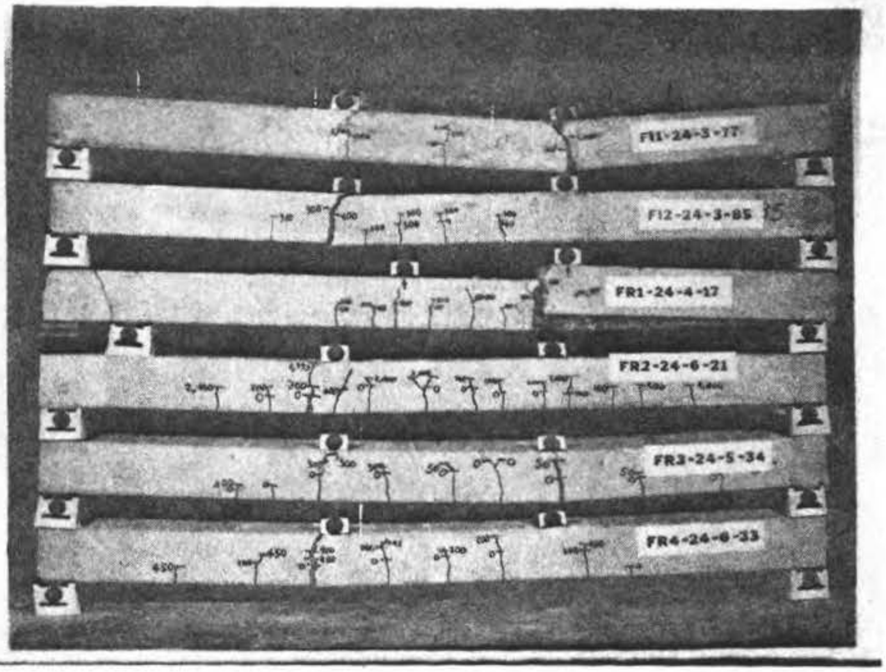

Fig. 8. Location and height of the cracks in all specimens.

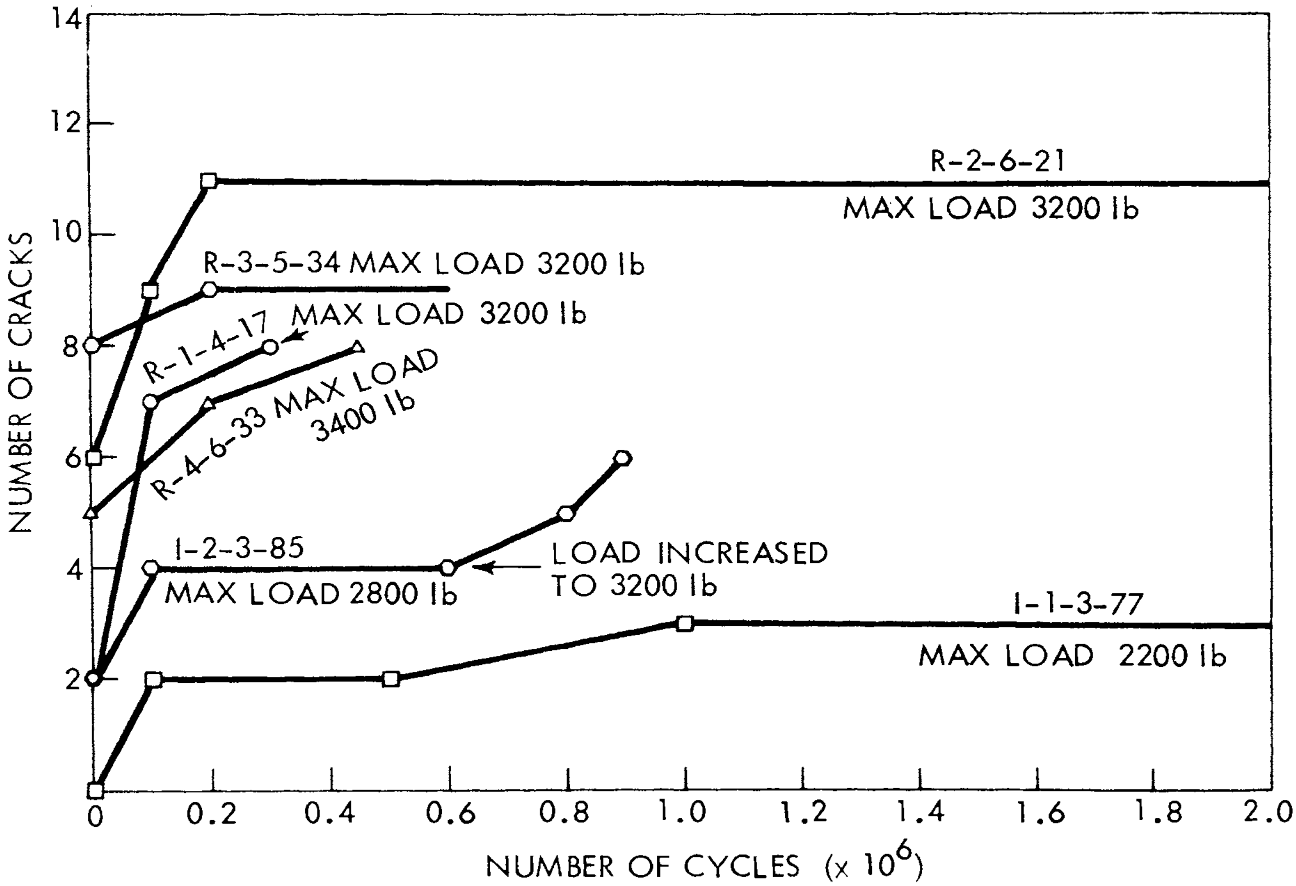

Fig. 9. Number of cracks vs number of cycles.

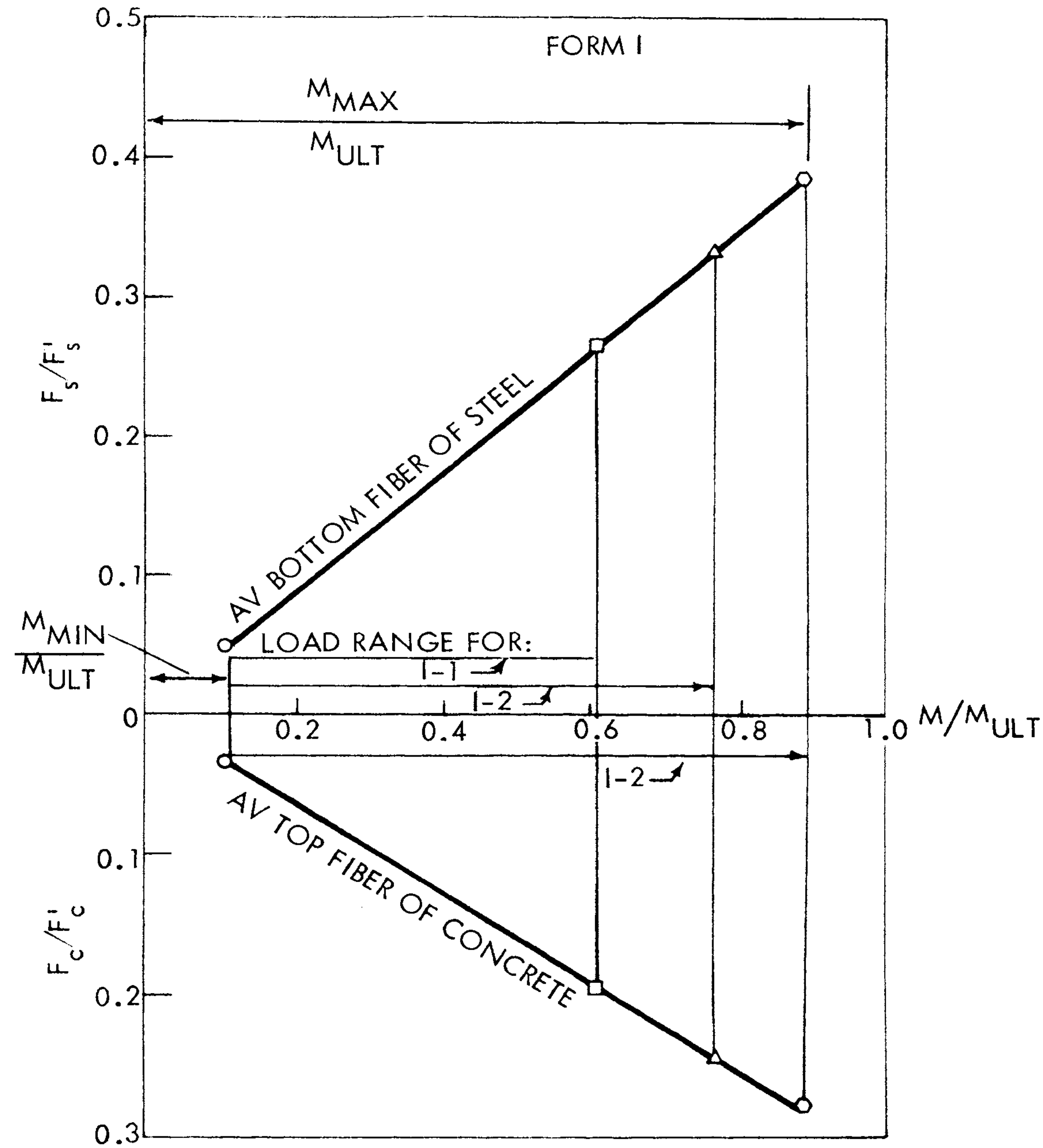

Fig. 10. Ratio of bending stresses to moment ratios for Form I.

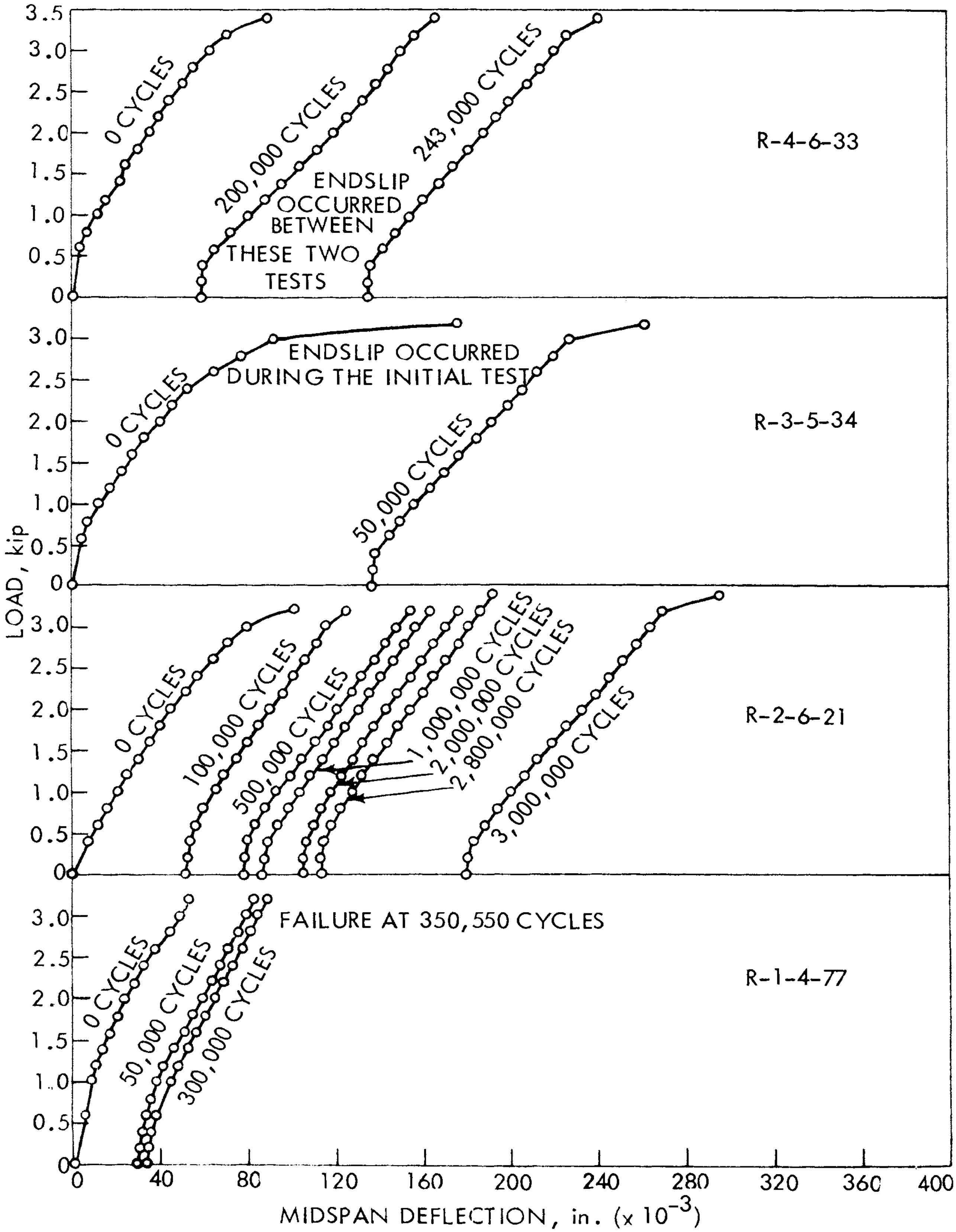

Fig. 11. Load vs midspan deflection for static tests.

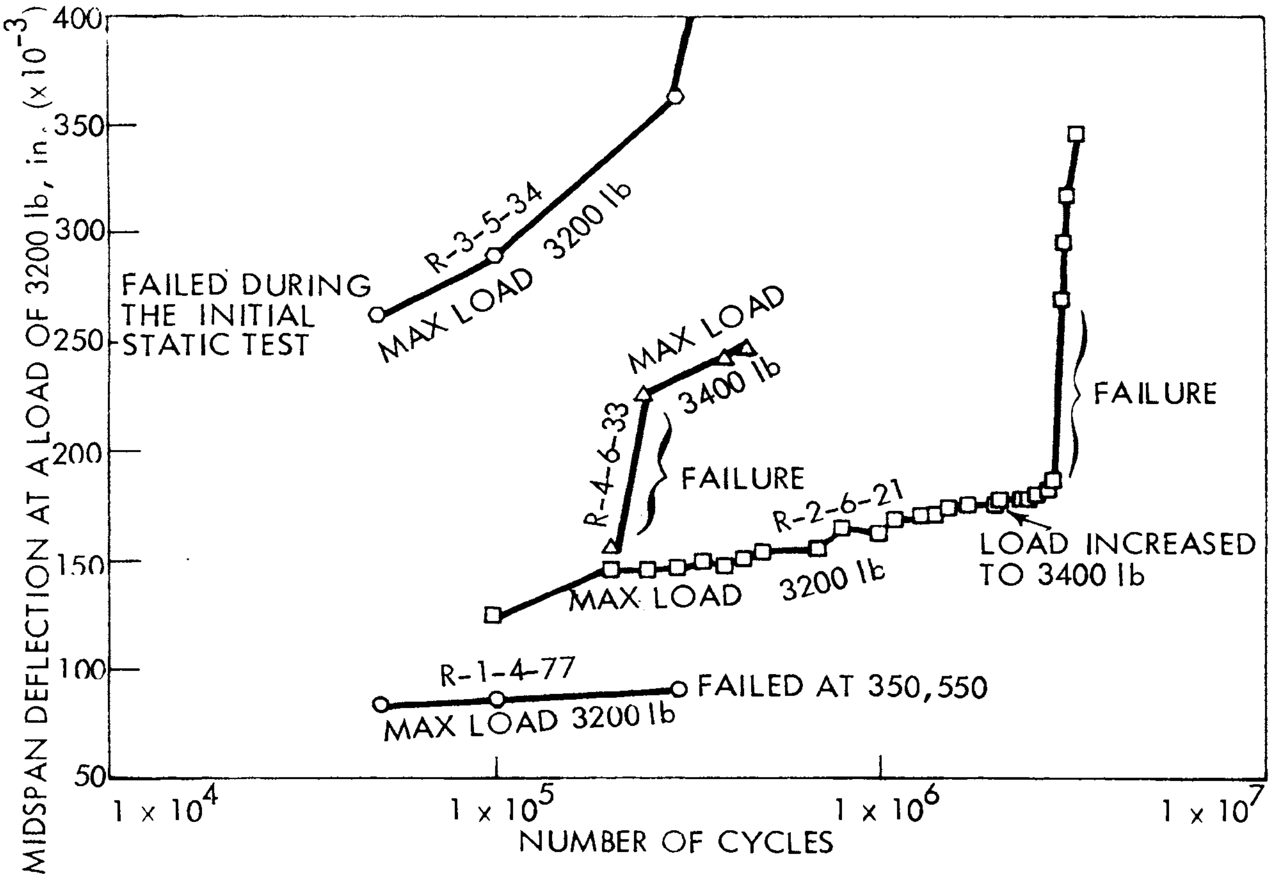

Fig. 12. Midspan deflection vs number of cycles for Form R.

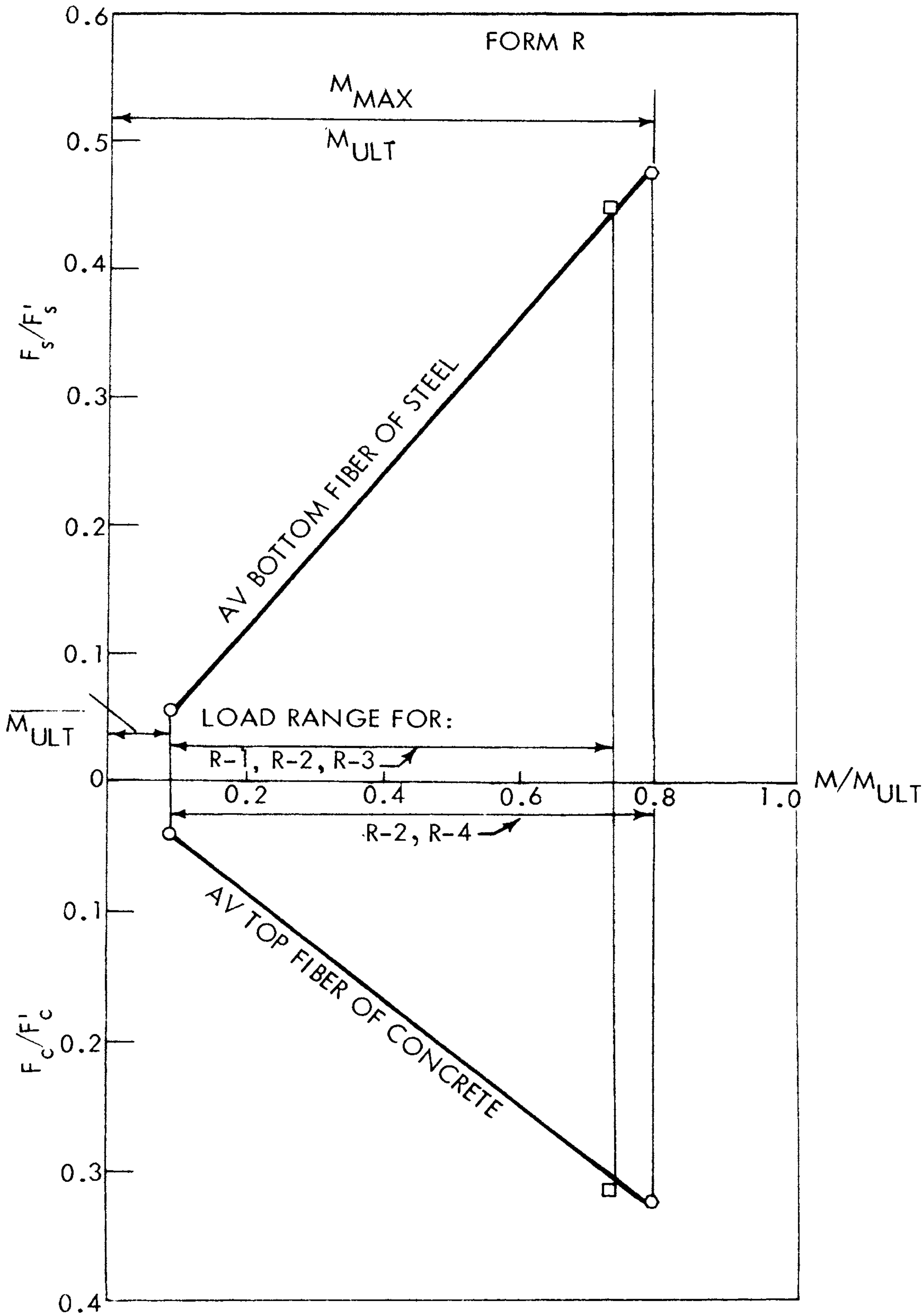

Fig. 13. Ratio of bending stresses to moment ratios for Form R.